

## Effects of Trace Lanthanum Ion on the Stability of Vaterite and Transformation from Vaterite to Calcite in an Aquatic System

Hiroshi Tsuno,<sup>\*,#</sup> Hiroyuki Kagi,<sup>†</sup> and Tasuku Akagi<sup>††</sup>

Doctoral Course in Agricultural Science, The United Graduate School, Tokyo University of Agriculture and Technology, Tokyo, 183-8509

<sup>†</sup> Laboratory for Earthquake Chemistry, Graduate School of Science, The University of Tokyo, Tokyo 113-0033

<sup>††</sup> Department of Environmental Natural Resource Science, Faculty of Agriculture, Tokyo University of Agriculture and Technology, Tokyo, 183-8509

(Received September 4, 2000)

The effect of lanthanum ion on the crystallization of calcium carbonate was investigated using  $\text{CaCl}_2\text{--NaHCO}_3$  solutions. A sampling vessel enabling us to sample a small aliquot of a solution at any time almost under a closed condition was invented for the experiments. The abundance of the crystallographic polymorphs in the precipitate was determined by powder X-ray diffraction. The formation of calcium carbonate from lanthanum-doped solutions can be featured by three stages: a spontaneous and rapid precipitation of vaterite, a transitive static stage and a delayed formation of calcite. Almost all lanthanum (> 95%) in the solution system (dissolved + suspended solid phases) was proved to be incorporated in the initially formed vaterite, and lanthanum in the vaterite seemed to be immobilized throughout the experiment. The presence of lanthanum in the starting solution ( $10^{-4}$  of calcium in mole) stabilized the initial vaterite crystal, preserved it much longer than one month and increased the solubility of  $\text{CaCO}_3$  to the level of vaterite. It is suggested that the lanthanum ion prohibited either the transformation initially formed vaterite to calcite or the overgrowth of calcite.

From the viewpoint of geochemistry and oceanography, it is curious that shallow water (water depths of a few hundred meters or less) of the oceans is supersaturated with respect to calcium carbonate ( $\text{CaCO}_3$ ). The supersaturation state ( $\Omega_{\text{calcite}}$ ) is higher than six with respect to calcite, and over four with respect to aragonite.<sup>1,2</sup> The supersaturation state of solution for calcite,  $\Omega_{\text{calcite}}$ , is defined as

$$\Omega_{\text{calcite}} \equiv \frac{a_{\text{Ca}^{2+}} \times a_{\text{CO}_3^{2-}}}{K_{\text{sp}(\text{calcite})}}, \quad (1)$$

where  $a_{\text{Ca}^{2+}}$  and  $a_{\text{CO}_3^{2-}}$  are the activities of free calcium ions and free carbonate ions. For a persuasive mechanism of the supersaturation, the incorporation of magnesium into carbonate<sup>3–5</sup> and the adsorption of organic matter<sup>6</sup> have been proposed. Recently, Akagi and Kono reported that a small amount of lanthanum ion ( $\text{La}^{3+}$ ) increased the solubility of calcium carbonate.<sup>7</sup> Under the assumption of chemical equilibrium, the presence of lanthanum ion ( $[\text{La}]/[\text{Ca}] = 7 \times 10^{-4}$ ) increased the ion activity products (IAP) of calcium carbonate by about 6 times as much as the lanthanum-free condition. Although the concentration of lanthanum in the experiment was far higher than those in actual seawater, the effects of the rare earth elements (REEs) might not be negligible, since REEs could be concentrated on the particles' surfaces due to their lack of chemically stable form in solution.

In order to achieve a precise description of the precipitation and dissolution of calcium carbonate, it is essential to understand both the carbonate ionic system in the solution and the solid-state structure of calcium carbonate. Carbonate ( $\text{CO}_3^{2-}$ ) and hydrogen carbonate ( $\text{HCO}_3^-$ ) ions are two typical dissolved species of carbon in an aquatic environment. An accurate description and prediction of the reactions occurring in the calcium carbonate system involves an extreme complication consisting of many parameters, such as equilibrium constants, activity coefficients, the concentrations of major and minor ions and ion pairs, the P-T condition, the surface condition, etc.<sup>8</sup> Moreover, the kinetics of the reactions is affected by minor chemical components, such as some organic matter<sup>9</sup> and various metal ions.<sup>10</sup>

Calcium carbonate has three crystal forms (vaterite, aragonite and calcite), with many variations of morphology in the natural minerals or organisms. The polymorphism of calcium carbonate has distinct physicochemical properties, including the crystal structures and morphology. The solubility of calcium carbonate decreases along with an increase in their thermodynamic stability, with calcite being the most stable and insoluble and vaterite being the most labile and soluble in the surface environment of the earth. The mechanisms controlling the polymorphism of calcium carbonate have attracted the interest of many researchers. In nature, aragonite, less stable than calcite, is often found to be stable in organisms like a shell or in hydrothermal deposits of hot springs, etc. It was reported that

<sup>#</sup> Present address: Laboratory for Earthquake Chemistry, Graduate School of Science, The University of Tokyo, Tokyo 113-0033.

less-stable polymorphs were preserved through kinetic effects<sup>11–14</sup> or were stabilized by impurities, such as some inorganic ions<sup>15</sup> and organic matters.<sup>16,17</sup> Several studies demonstrated that the initial spontaneous precipitation was vaterite at high supersaturation of approximately 7 in  $\Omega$ .<sup>11,18,19</sup> In the case of a particularly high supersaturation state ( $\Omega_{\text{calcite}}$  was about 4600), the initial spontaneous precipitation is amorphous calcium carbonate.<sup>11</sup> Taking account of the difference in the physicochemical properties in the three polymorphs of calcium carbonate, as mentioned above, one can expect that the increase in the solubility induced by the lanthanum ion was closely related to the morphology and/or polymorphism of calcium carbonate.

To elucidate the solubility change by lanthanum reported by Akagi and Kono,<sup>7</sup> a study of polymorphism occurring in the solution is necessary. In the present work, we invented a reaction vessel which enabled us to sample a solution almost under closed condition; the relationship between the chemical state of solutions and polymorphism of the precipitate could then be studied in detail.

## Experimental

**A. Precipitation of Calcium Carbonate.** The initial supersaturation state ( $\Omega_{\text{calcite}}$ ) of the starting solution was prepared at approximately 40. The experiments were conducted in a closed system. Consequently, the total amount of carbon within the system was constant, which allowed an arithmetic analysis of the carbonic acid system.<sup>7</sup> The amount of the precipitate and IAP of calcium carbonate were calculated from the pH of the solutions based on the assumption of chemical equilibrium among the ionic species in solutions. The reacting vessel invented in this study (Fig. 1) had a

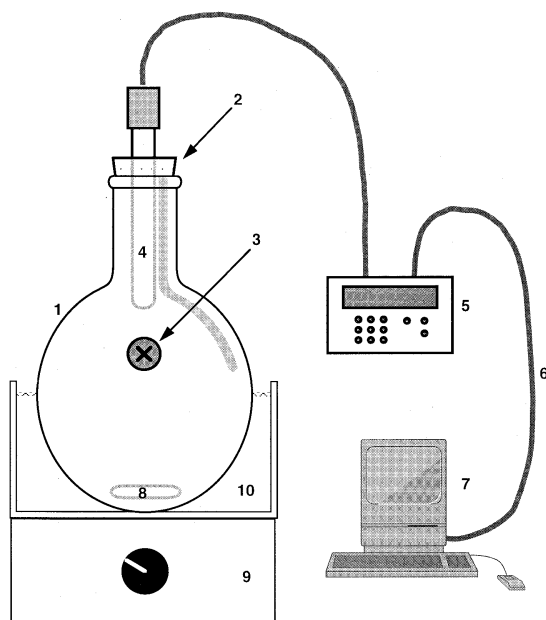


Fig. 1. Schematic diagram of the experimental apparatus. 1: glass vessel, 2: silicon rubber stopper, 3: silicon rubber septum, 4: pH electrode (pH, temperature), 5: pH meter, 6: RS232C connection, 7: personal computer; auto recording pH, temperature and time, 8: magnetic stirring bar coated with Teflon, 9: magnetic stirrer, 10: thermostatic water bath

sampling rubber-septum through which small aliquots of solution (about 100–300  $\mu\text{L}$ ) were sampled using a syringe.

Starting solutions of lanthanum(III) chloride, calcium chloride and sodium hydrogen carbonate were prepared by dissolving analytical-grade reagents (Wako) with milli-Q<sup>®</sup> water, respectively. After calcium chloride (with given amount of lanthanum doped) and sodium hydrogen carbonate (with given amount of lanthanum doped) solutions were mixed, the mixture was stirred for one minute. The mixture (referred to as a starting solution hereafter) was transferred into the vessel and immediately sealed with a silicon rubber stopper in which a pH electrode was embedded (Fig. 1). The pH meter used in this study consisted of a combination pH electrode and temperature sensor. The data of the pH, temperature and reaction time were sent to a personal computer. The amount of precipitate and IAP were calculated from the initial concentrations of all the chemical species in the system and pH at each sampling time according to a previously reported method<sup>7</sup> (see Appendix). The temperature of the solutions was at room temperature (Exp. #1–#8 on Table 1) or was kept at 30  $^{\circ}\text{C}$  by a thermostated water bath (Exp. #9–#12 on Table 1). We neglected the small amount of  $\text{CO}_2$  (gas) produced during the experiments. Stirring was applied using a magnetic stirrer during the experiments, which was not done in the experiments by Akagi and Kono.<sup>7</sup> The compositions of the starting solutions are listed in Table 1. The highest pH of the solution was estimated to be around 8.3 from a calculation of the carbonate system equilibria of the solution which had produced no precipitation. Even though all lanthanum was in the form of  $\text{La}^{3+}$ , the concentration of  $\text{OH}^-$  under this condition was too low to precipitate  $\text{La}(\text{OH})_3$  ( $K_{\text{sp}} = 1.7 \times 10^{-19}$  by Moeller and Fogel<sup>20</sup>) at the highest pH just after mixing. The two major chemical species of the dissolved lanthanum in the starting solution were  $\text{LaCO}_3^+$  and  $\text{La}(\text{CO}_3)_2^-$ , and the amounts of three hydroxide complexes ( $\text{LaOH}^{2+}$ ,  $\text{La}(\text{OH})_2^+$ ,  $\text{La}(\text{OH})_3^0$ ) were negligibly small compared with the two major species (calculations were performed using constants reported by Lee and Bayne<sup>21</sup>;  $\text{CO}_3\beta_1(\text{La}) = 10^{7.12}$ ,  $\text{CO}_3\beta_2(\text{La}) = 10^{11.59}$ ,  $\beta_1^*(\text{La}) = 10^{-8.66}$ ,  $\beta_2^*(\text{La}) = 10^{-18.14}$  and  $\beta_3^*(\text{La}) = 10^{-27.90}$ , where  $\beta_n^*(\text{La}) = \text{OH}\beta_n(\text{La}) \times K_{\text{w}}^n$  and  $K_{\text{w}} = [\text{H}^+][\text{OH}^-]$ ).

During the experiment, a sample solution (0.2 ml) including suspended precipitates was sampled using a 2.5 ml syringe equipped with a membrane filter with a pore size of 0.45  $\mu\text{m}$  (Millipore<sup>®</sup> SLHVL040S). The precipitate on the filter was rinsed with distilled water and dried at room temperature.

**B. Observation and Analysis of the  $\text{CaCO}_3$  Precipitate.** For powder X-ray diffraction (XRD) and scanning electron microscopy (SEM) image observations, the precipitate was recovered from the filter cartridge. A platinum coating was produced on the specimens to avoid any charge-up; secondary electron images were observed with a scanning electron microscope (SEM, JEOL JSM-6000F) with an acceleration voltage of 3.0 kV and an emission current of 8.0  $\mu\text{A}$ .

Polymorphs of calcium carbonate were determined with a powder X-ray diffraction photograph using a 114 mm diameter Gandolfi camera with the  $\text{Cu } K\alpha$  line. The photographic density (blackening) of an X-ray film was scanned by a microdensitometer. The composition of the polymorphs was determined through an accurately integrated intensity of characteristic diffraction lines of calcite (104),  $I_{\text{c}}$ , and vaterite (110),  $I_{\text{v}}$ , on a powder photograph. The conversion of the ratio ( $I_{\text{v}}/(I_{\text{c}} + I_{\text{v}})$ ) to weight percent of calcite was achieved by using a calibration curve reported by Spanos and Koutsoukos.<sup>19</sup>

The precipitate in the syringe filter cartridge was dissolved with

Table 1. The Concentration of Starting Solutions and the Results of CaCO<sub>3</sub> Precipitation Experiments

Exp. No.	Initial solution				Time during metastable stage <sup>a)</sup> /min	Calculated log IAP Equilibrium <sup>b)</sup> (metastable) <sup>c)</sup>	Temperature during the reactions minimum - mean - maximum /°C
	[Σ CO <sub>2</sub> ]/mmol kg <sup>-1</sup>	[Ca]/mmol kg <sup>-1</sup>	[La]/μmol kg <sup>-1</sup>	La/Ca			
1	14.4	15.5	0	0	—	-8.4	21.7 - 24.8 - 26.3
2	15.0	16.0	7.8	4.9×10 <sup>-4</sup>	180-630	-7.9 (-7.2)	21.0 - 26.1 - 27.2
3	14.8	15.7	7.9	5.0×10 <sup>-4</sup>	240-720	-7.9 (-7.2)	21.2 - 25.7 - 27.0
4	14.2	14.4	0	0	—	-8.6	28.4 - 29.1 - 30.5
5	13.8	13.8	8.4	6.1×10 <sup>-4</sup>	50-465	-8.1 (-7.4)	26.8 - 29.3 - 30.7
6	14.2	14.1	17.3	1.2×10 <sup>-3</sup>	50-500	-8.0 (-7.4)	27.5 - 29.2 - 30.5
7	14.6	14.5	8.9	6.1×10 <sup>-4</sup>	90-640	-8.0 (-7.3)	27.0 - 28.5 - 29.6
8	14.8	14.7	8.9	6.1×10 <sup>-4</sup>	50-410	-7.9 (-7.4)	25.6 - 29.0 - 31.6
9	15.4	15.4	0	0	—	-8.6	28.7 - 29.9 - 30.0
10	15.6	15.4	0	0	—	-8.6	28.3 - 29.9 - 30.2
11	15.1	15.0	9.1	6.0×10 <sup>-4</sup>	50-350	-7.9 (-7.4)	28.7 - 30.0 - 30.1
12	15.1	15.0	9.2	6.1×10 <sup>-4</sup>	70-330	-8.0 (-7.3)	28.4 - 30.2 - 30.5

a) Figures stands for the time from the beginning of the reaction. b) Calculated from the pH value after 1400 min from the beginning of the reaction, assuming that pH is an equilibrium pH. c) Calculated from the average pH value of the metastable stage.

nitric acid, and a known amount of indium solution was added as an internal standard, and was finally diluted to 0.4 M HNO<sub>3</sub> with milli-Q water (1 M = 1 mol dm<sup>-3</sup>). The filtrate of the cartridge was also treated by the same procedure. The concentration of lanthanum in the final solutions was measured using an inductively coupled plasma mass spectrometer (ICP-MS, VG Plasma Quad). The concentration of calcium in the final solutions was analyzed with an inductively coupled plasma atomic emission spectrometer (ICP-AES, SII SPS1200). The lanthanum concentration in the precipitate was evaluated from the La/Ca ratio.

## Results and Discussion

**A. Formation of Calcium Carbonate Precipitate.** Typical examples of the pH change during the experiments with and without lanthanum ion are shown in Fig. 2. The decrease in the pH was caused by the precipitation of calcium carbonate. The amount of precipitated CaCO<sub>3</sub> was calculated from the pH of the solution, assuming chemical equilibrium in a closed sys-

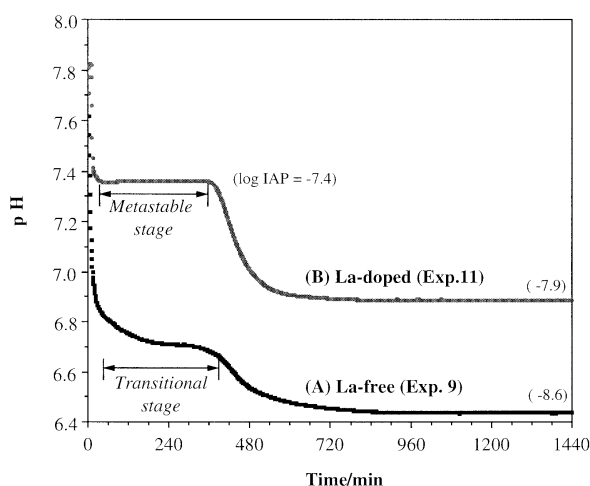


Fig. 2. Plots of pH change with time during the crystallization in a solution without lanthanum (Exp. 9) (A) and a solution with lanthanum (Exp. 11) (B). The calculated log IAP values of calcium carbonate in the solutions of the metastable stage and equilibrium were indicated in parentheses.

tem; the precipitate was found to increase with time (Fig. 5). In all experiments, the pH became almost constant after one day (1440 min).

In the case of a lanthanum-free system, the pH change became sluggish, but did not remain constant (100–300 min), in contrast to the case of the lanthanum-doped system described later. The calculated log IAPs after one day from the starting point of the experiments were usually about -8.5 (see Table 1). These values were close to the reported log  $K_{sp}$  for calcite (-8.48<sup>22</sup>; -8.480 at 25 °C<sup>23</sup>). This result strongly suggests that the solutions without the addition of lanthanum were close to being in equilibrium with calcite after one day.

When lanthanum ion was doped in the initial supersaturated solution, a remarkable change in the transitional stage was observed. As can be seen in Fig. 2, a static pH period (metastable stage) without exhibiting a decrease in the pH appeared at between 50 and 350 min. The log IAP of calcium carbonate during the metastable stage was calculated from the pH value assuming chemical equilibrium within a system of CO<sub>2</sub>-HCO<sub>3</sub><sup>-</sup>-CO<sub>3</sub><sup>2-</sup>. The calculated log IAP was in the range of -7.2 to -7.4 (see Table 1). After the metastable stage, another precipitation started and the carbonic acid system reached a new equilibrium. If we assume that the carbonic acid system in the lanthanum-doped solution after one day was in equilibrium, the ion activity products (IAP) of calcium carbonate could also be calculated from the pH. The calculated log IAP was in the range of -7.9 to -8.1 independent of the concentration of lanthanum in the starting solutions (Table 1). This value is close to the reported value of vaterite (-7.902 at 25 °C<sup>23</sup>). The presence of vaterite was confirmed from the X-ray diffraction pattern, as described later. It is noteworthy that the system kept vaterite for a long period of more than one month in spite of the thermodynamically labile characteristics of vaterite.

We carried out several experiments with (Exp. #9–#12) and without any temperature control (Exp. # 1–#8), obtaining almost identical results. We consider that the effect of temperature is not noticeably important in the temperature range of the present experiments.

Experiments by Akagi and Kono,<sup>7</sup> in which no stirring was

applied, showed no metastable stage, and the pH of lanthanum-doped solution of their experiment reached only that of the metastable stage in the present study. We reexamined their results using the reaction vessel without stirring, and obtained results similar to theirs (data not shown).

**B. Crystal Shapes and Polymorphism of Calcium Carbonate.** Typical SEM images of the precipitate are shown in Fig. 3. The precipitate occurring at an early stage in the experiments was spherulite, indicating the aggregation of particulates

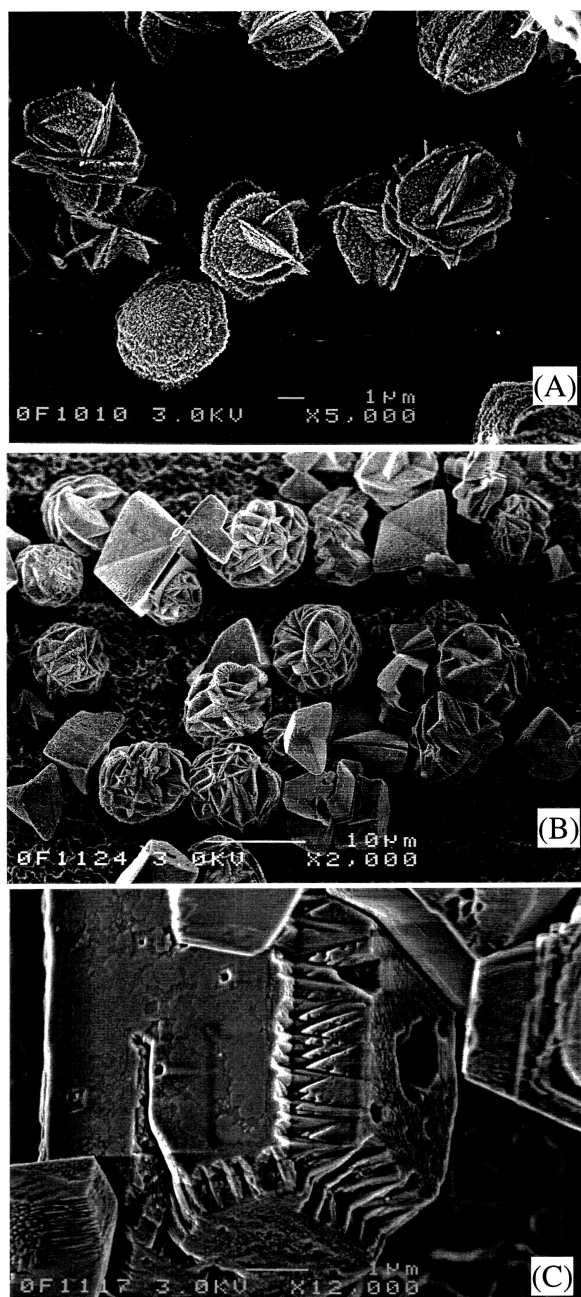


Fig. 3. Typical scanning electron microscope images of precipitate. (A) sampled from a La-free solution at 15 min from the beginning of the reaction. (B) (C) sampled from a La-doped solution at 110 min (B) and 1320 min (C) from the beginning of the reaction.

with a few-hundred nanometer size for both the lanthanum-free system (Fig. 3A) and the lanthanum-doped system (Fig. 3B). The spherulite transformed to the euhedral shape of calcite in the case of the lanthanum-free condition. These observations are consistent with the morphology of calcium carbonates precipitated in aquatic solutions numerically reported.<sup>11,12,18,19</sup> When lanthanum was added to the starting solution, spherulite became more persistent and survived during the metastable stage (Fig. 3B); it then turned to rhombohedral calcite shape, which showed a derangement in the crystal surface (Fig. 3C).

Figure 4 shows typical X-ray diffraction profiles measured after several time intervals. The profiles exhibit an obvious difference between lanthanum-free and lanthanum-doped systems with time. Figure 5 shows the time dependencies of the polymorphic abundance both for the lanthanum-free system and the lanthanum-doped system. The observed difference is discussed later in detail.

**C. Lanthanum Concentration in the Precipitate and Solutions.** The time dependencies of the lanthanum amount in the liquid and solid fractions are shown in Fig. 6. The concentration of lanthanum in the solution decreased rapidly at the very beginning of the reaction, and then gradually declined to nearly 1/100 of the concentration in the starting solution ( $1.6 \times 10^{-1} \mu\text{mol kg}^{-1}$ , an average value in 900–1400 min of Exp. 11), which was as low as the detection limit of the adopted method. On the other hand, the lanthanum amount in the precipitate increased quickly until the first one hour of the reaction, and remained almost constant thereafter ( $4.3 \mu\text{mol kg}^{-1}$ , an average value in 900–1400 min of Exp. 11). The sum of the lanthanum amounts in the solution and precipitate at the final stage ( $4.4 \mu\text{mol kg}^{-1}$ , an average value in 900–1400 min of Exp. 11), however, explained only half of the lanthanum amount initially given to the system ( $9.1 \mu\text{mol kg}^{-1}$ , Exp. 11). We suspected that the rest of the lanthanum was adsorbed onto the wall of the glass reactor as soon as the starting solution was transferred into it. The silanol group on the surface of glass induces dissolved species of lanthanum (especially  $\text{La}^{3+}$ ) to adsorb on glass surface. We prepared a silanized vessel with dimethyldichlorosilane in order to substitute a methyl-terminated surface for the adsorptive silanol surface. Using the surface-terminated vessel, the obtained results corresponded to the case using an untreated vessel with twice the concentration of lanthanum in the starting solutions (unpublished data). This suggests that approximately half of the lanthanum in the system (solution + precipitate) in the present experiments was adsorbed on the glass surface. Thus, more than 95% of the lanthanum in the solution system (dissolved + suspended solid phases, excluding the missing lanthanum) was incorporated into the precipitate, which is attributed to vaterite in the later discussion.

**D. The Crystallization of  $\text{CaCO}_3$  in the Lanthanum-Free System.** Without the lanthanum ion in the starting solution, calcium carbonate immediately precipitated as thermodynamically unstable vaterite. As the reaction proceeded, vaterite (spherulite) transformed to euhedral calcite. As can be seen from Fig. 5A, during the transformation from vaterite to calcite, the precipitation rate of calcium carbonate was relatively

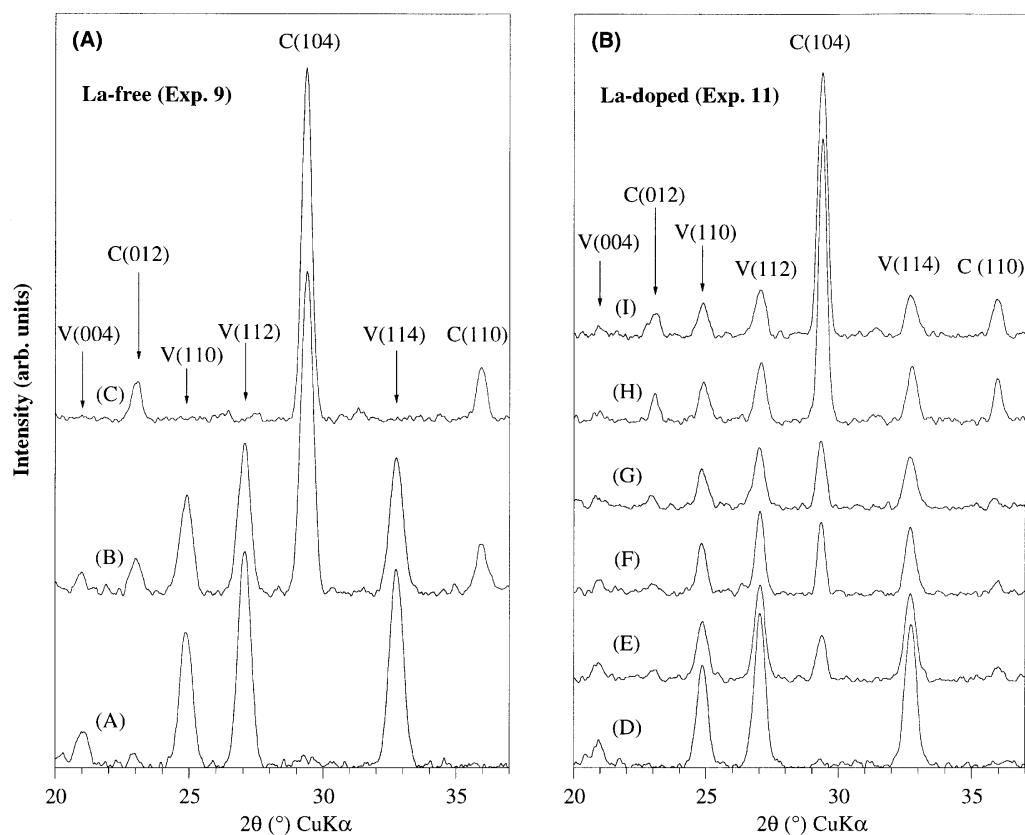


Fig. 4. Chronological change of X-ray diffraction profiles. (A–C): Precipitate sampled from a solution without lanthanum (Exp. 9). After 16 min (A), 202 min (B) and 520 min (C) from the beginning of the reaction. (D–I): Precipitate sampled from a solution with lanthanum (Exp. 11). After 10 min (D), 27 min (E), 380 min (F), 398 min (G), 633 min (H) and 4755 min (I) from the beginning of the reaction.

slower than before and after the period of transformation (transitional stage in Fig. 2A). Once most of the vaterite transformed to calcite, calcium carbonate precipitated quickly to reach equilibrium (see Fig. 5). The transformation from vaterite to calcite began after a few minutes from the mixing of the two solutions and completed in 8–10 hours. The vaterite spontaneously nucleated at the beginning of the experiments was always spherulite (about 5  $\mu\text{m}$  in diameter, see Fig. 3A). Ogino et al.<sup>11</sup> reported that the spherical vaterite gradually transformed to rhombohedral calcite during the transition. In their case, highly supersaturated solutions of  $\text{Ca}^{2+}$  and  $\text{CO}_3^{2-}$  ions rapidly precipitated as amorphous calcium carbonate, and transformed to a crystalline calcium carbonate polymorphs within several minutes followed by the phase transformation from vaterite to calcite in a temperature range between 14 and 30  $^{\circ}\text{C}$ . On the contrary to the experiments by Ogino et al.,<sup>11</sup> amorphous  $\text{CaCO}_3$  was not observed in this study. This is because  $\Omega_{\text{calcite}}$  of the starting solutions was around 40 in this study, whereas that in the work of Ogino et al. was about 4600.<sup>11</sup> Their supersaturation was one hundred-times as high as ours and may have been sufficient to create high supersaturation state necessary for precipitating amorphous calcium carbonate.

**E. Inhibition of Transformation of Vaterite to Calcite by Lanthanum Ion.** As can be seen from Fig. 5B, in the first

tens of minutes, vaterite formation occurred quickly and calcite formation was not observed. During the metastable stage, the composition as well as the amount of polymorphs was constant. After the metastable stage, a break point of the calcite formation was observed. Transiting the break point, calcium carbonate precipitated as calcite exclusively. The amount of initially formed vaterite was almost constant throughout the experiment, even after calcite formed.

The concentration of lanthanum was very low (around  $1 \times 10^{-7} \text{ mol kg}^{-1}$ ) in the solution during the reaction, except for the very early stage of the reaction in which the concentration of the starting solution was reflected (Fig. 6). On the other hand, the amount of lanthanum in the precipitate was relatively high and remained almost constant during the reaction. The La/Ca ratio in the whole precipitate (Fig. 7A) dropped abruptly at the break point. Taking into consideration that most of the precipitate formed after the metastable stage was calcite, and that the total amount of lanthanum in the precipitate was almost constant during the experiment, we judged that lanthanum was concentrated exclusively in vaterite. Based on this assumption, the La/Ca ratio in vaterite can be calculated from the polymorphic abundance and the concentration of lanthanum in the precipitate. The calculated La/Ca ratio in vaterite (Fig. 7B) was virtually constant during the reaction where the large gap around the break point was much subdued to the level within

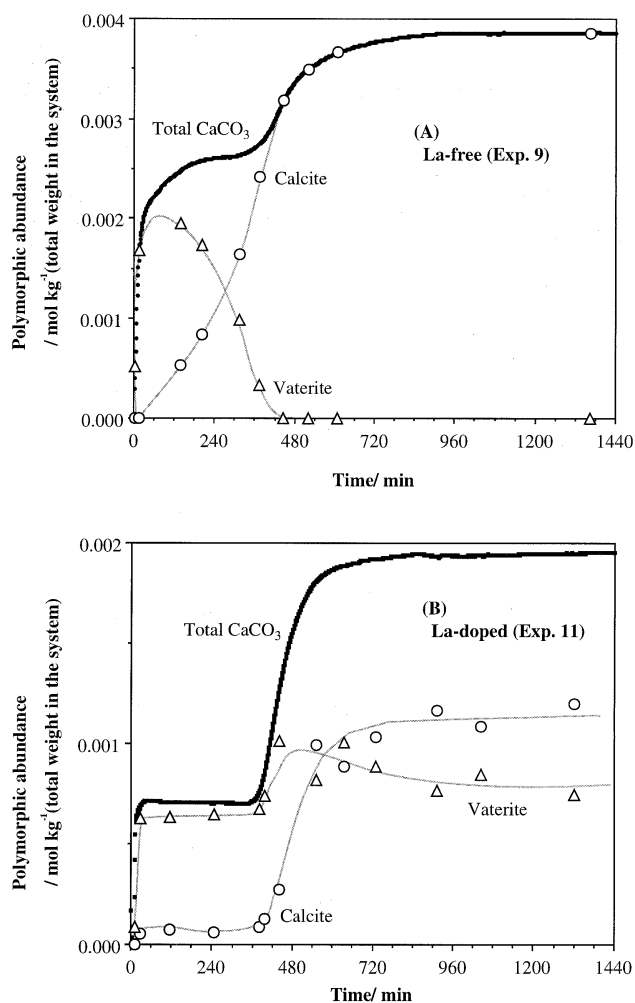


Fig. 5. Typical change of the polymorphic abundance in a solution without lanthanum (Exp. 9) (A) and a solution with lanthanum (Exp. 11) (B).  $\Delta$ : Vaterite,  $\circ$ : Calcite, and  $\bullet$ : Total  $\text{CaCO}_3$ . Total  $\text{CaCO}_3$  was calculated from pH and given concentration of chemical species in the starting solutions.

analytical error due to the uncertainty of parameters involved in the calculation.

Spanos and Koutsoukos<sup>19</sup> reported on the dependence of the transformation from vaterite to calcite upon supersaturation. According to their report, the transformation of the initially formed vaterite to calcite took place through the dissolution of more soluble vaterite. At supersaturation states of 2.3 to 4.4, the transformation was controlled by the dissolution of vaterite, whereas at lower supersaturation states ( $\Omega$  was in the range of 1.2 to 2.3) the dissolution rate of vaterite was comparable with the rate of calcite crystallization. The supersaturation state in the present study was higher than 4, and it can be suggested from their study that the vaterite dissolution could be the rate-determining step of the calcite formation in our study.

The transformation of the labile phase to the most stable calcite is also influenced by the minor or trace impurities. The presence of phosphate ions ( $5 \times 10^{-2} \mu\text{mol kg}^{-1}$ ) in the precipitating solution stabilized the initially formed vaterite by a re-

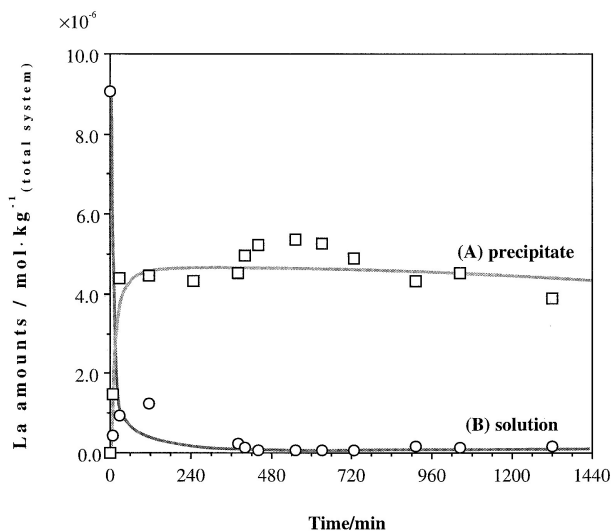


Fig. 6. Change in the lanthanum amounts of the precipitate and the solution sampled from the lanthanum-doped starting solution (Exp. 11). The lanthanum amount of each phase was described as their relative abundance by total system.  $\Delta$ : The lanthanum amounts of the solution.  $\square$ : The lanthanum amounts of the precipitate.

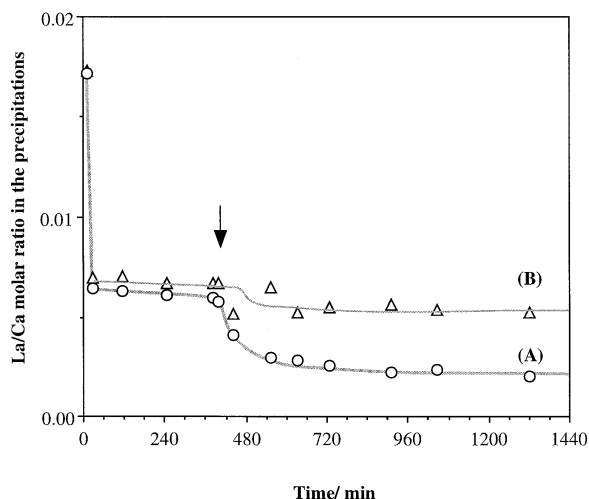


Fig. 7. Change in the La/Ca molar ratio in the precipitate sampled from the lanthanum-doped starting solution (Exp. 11). The observed La/Ca ratio of total precipitate (A) and the calculated La/Ca ratio of vaterite (B), assuming that lanthanum was concentrated only in vaterite. The arrow in the figure indicates the time of the break point observed in Fig. 5B (see text).

markable decrease in the transformation rate to calcite.<sup>24</sup> The stabilization of vaterite by the presence of the phosphate ions was ascribed to the retardation of both the dissolution of vaterite and the crystallization of calcite, caused by blocking of the active sites for the dissolution of vaterite and for the crystallization of calcite by the absorbed phosphate. By an analogy to the case of phosphate, our present result suggests that lanthanum ions block the active sites on vaterite dissolution and cal-

cite crystallization.

### Conclusions

The small amount of lanthanum ions in the supersaturated parent solutions of the calcium carbonate was found to disturb the formation of calcium carbonate in the following ways;

A. The parent solutions containing lanthanum induced an evident metastable stage, where the abundance of the polymorphs and La/Ca ratios in the precipitate did not change.

B. They also produced persisting vaterite which survived more than one month.

C. Most of lanthanum was quickly incorporated into the initially formed vaterite.

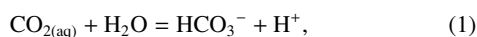
D. Lanthanum in the initially formed vaterite is considered to prohibit a transformation to calcite.

Zhong and Mucci<sup>25</sup> reported that REEs were strongly partitioned into calcite and substituted for calcium ion with a partition coefficient of  $10^{3.6}$ . Facing the strong mutual association among REEs, calcium and carbonate ions in nature and also shown in this study, it could be important to understand how REEs may affect the carbonic acid system. The effect of lanthanum ion on the crystallization of  $\text{CaCO}_3$  might provide a possible explanation for the supersaturation of calcium carbonate in seawater.

We are grateful to Dr. Okada, Dr. Fu and Ms. Yabuki for full access to the Gandolfi camera, X-ray source and ICP-MS at RIKEN institute. We are indebted to Prof. Nakamuta, Kyusyu University, for the digitization of X-ray photographs. We thank Prof. Dokiya, Tokyo University of Agriculture and Technology, and Prof. Fukami, Utsunomiya University, for their encouragement and useful advice of the research. Analysis and display of X-ray powder diffraction pattern were performed on a Macintosh computer using the public domain MacDiff 4.0.9a (developed by Dr. Rainer Petschick, Geologisch-Paläontologisches Institut, Johann Wolfgang Goethe-Universität Frankfurt am Main). The manuscript was greatly improved by the comments from two anonymous reviewers. This research was financially supported by Nissan Science Foundation.

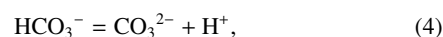
### Appendix

Dissociation reactions of carbonic acids, ion-pairing reactions between major cations ( $\text{Na}^+$  and  $\text{Ca}^{2+}$ ) and anions ( $\text{HCO}_3^-$  and  $\text{CO}_3^{2-}$ ) and between  $\text{La}^{3+}$  and  $\text{CO}_3^{2-}$  are considered. They were summarized as follows along with the equilibrium constant of each reaction used in the calculations:



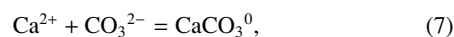
$$K_1 = \frac{\gamma_{\text{HCO}_3^-} [\text{HCO}_3^-] 10^{-\text{pH}}}{[\text{CO}_{2(\text{aq})}]}, \quad (2)$$

$$\log K_1 = -356.3094 - 0.06091964T + 21834.37/T + 126.8339 \log T - 1684915/T^2, \quad (3)$$



$$K_2 = \frac{\gamma_{\text{CO}_3^{2-}} [\text{CO}_3^{2-}] 10^{-\text{pH}}}{\gamma_{\text{HCO}_3^-} [\text{HCO}_3^-]}, \quad (5)$$

$$\log K_2 = -107.8871 - 0.03252849T + 5151.79/T + 38.92561 \log T - 563713.9/T^2, \quad (6)$$



$$K_{\text{Ca}^{2+}-\text{CO}_3^{2-}} = \frac{\gamma_{\text{CaCO}_3^0} [\text{CaCO}_3^0]}{\gamma_{\text{Ca}^{2+}} [\text{Ca}^{2+}] \gamma_{\text{CO}_3^{2-}} [\text{CO}_3^{2-}]}, \quad (8)$$

$$\log K_{\text{CaCO}_3^0} = -1228.732 - 0.299444T + 35512.75/T + 485.818 \log T, \quad (9)$$



$$K_{\text{Ca}^{2+}-\text{HCO}_3^-} = \frac{\gamma_{\text{CaHCO}_3^+} [\text{CaHCO}_3^+]}{\gamma_{\text{Ca}^{2+}} [\text{Ca}^{2+}] \gamma_{\text{HCO}_3^-} [\text{HCO}_3^-]}, \quad (11)$$

$$\log K_{\text{CaHCO}_3^+} = 1209.120 + 0.31294T - 34765.05/T - 478.782 \log T, \quad (12)$$



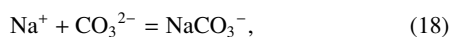
$$K_X = \gamma_{\text{Ca}^{2+}} [\text{Ca}^{2+}] \gamma_{\text{CO}_3^{2-}} [\text{CO}_3^{2-}], \quad (14)$$

$$\log K_{\text{calcite}} = -171.9065 - 0.0779933T + 2839.319/T + 71.595 \log T, \quad (15)$$

$$\log K_{\text{aragonite}} = -171.9773 - 0.0779933T + 2903.293/T + 71.595 \log T, \quad (16)$$

$$\log K_{\text{vaterite}} = -172.1295 - 0.0779933T + 3074.688/T + 71.595 \log T, \quad (17)$$

where  $\gamma_i$  is the activity coefficient of an ion  $i$ ,  $x$  is polymorphs of calcium carbonate and  $T$  is in °K (available over the range of 0 to 90 °C (Eqs. 12, 13, 14 and 15), 5 to 80 °C (Eq. 9) and 0 to 100 °C under 1 atm. total pressure (Eqs. 3 and 6)). The equations and constants were reported by Plummer and Busenberg.<sup>23</sup>



$$K_{\text{Na}^+ - \text{CO}_3^{2-}} = \frac{\gamma_{\text{NaCO}_3^-} [\text{NaCO}_3^-]}{\gamma_{\text{Na}^+} [\text{Na}^+] \gamma_{\text{CO}_3^{2-}} [\text{CO}_3^{2-}]}, \quad (19)$$

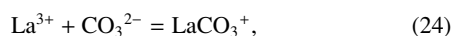
$$\log K_{\text{NaCO}_3^-} = 1.02 \quad \text{at } 25^\circ\text{C}, \quad (20)$$



$$K_{\text{Na}^+ - \text{HCO}_3^-} = \frac{\gamma_{\text{NaHCO}_3^0} [\text{NaHCO}_3^0]}{\gamma_{\text{Na}^+} [\text{Na}^+] \gamma_{\text{HCO}_3^-} [\text{HCO}_3^-]}, \quad (22)$$

$$\log K_{\text{NaHCO}_3^0} = -0.19 \quad \text{at } 25^\circ\text{C}, \quad (23)$$

The values of ion-pair formation of sodium were reported by Millero and Schreiber.<sup>20</sup>



$$K_{\text{La}^{3+} - \text{CO}_3^{2-}} = \frac{\gamma_{\text{LaCO}_3^+} [\text{LaCO}_3^+]}{\gamma_{\text{La}^{3+}} [\text{La}^{3+}] \gamma_{\text{CO}_3^{2-}} [\text{CO}_3^{2-}]}, \quad (25)$$

$$\log K_{\text{LaCO}_3^+} = 7.12 \quad \text{at } 25^\circ\text{C}, \quad (26)$$

The formation constant of lanthanum-carbonate complex was taken from Lee and Byrne.<sup>21</sup> According to their calculation, the presence of any hydrated species of lanthanum ions can be neglected in our experiments.

The closed system constrains the amount of the total carbonic species to be constant, i.e.

$$\begin{aligned} & [\text{CO}_{2(\text{aq})}] + [\text{HCO}_3^-] + [\text{CO}_3^{2-}] + [\text{NaHCO}_3^0] + [\text{NaCO}_3^-] \\ & + [\text{CaHCO}_3^+] + [\text{CaCO}_3^0] + [\text{LaCO}_3^+] + \text{CaCO}_{3(\text{precipitation})} \\ & = \text{constant}. \end{aligned} \quad (27)$$

The concentrations of all the chemical species appearing in the reactions are uniquely determined for the given amounts of total carbon, calcium, sodium and lanthanum, if one of any concentrations of the species appeared in the chemical equilibrium equations listed above is known. When equilibrium is extended to the reaction of CaCO<sub>3</sub> formation, K<sub>sp</sub> is also obtained from the calculated concentrations of carbonate and calcium ions. The activity coefficients of ions in the solutions (molar ionic strength,  $I < 0.06$ ) were given by the Davies equation<sup>8</sup>, i.e.

$$\log \gamma_i = -0.5z_i^2 \left\{ \frac{\sqrt{I}}{1 + \sqrt{I}} - 0.2I \right\} \left\{ \frac{298}{T} \right\}, \quad (28)$$

where  $z_i$  is the charge number of an ion  $i$ ,  $T$  is the temperature in °K

(available over the range of about 0 to 50 °C) and  $I$  is the dimensionless ionic strength of the solution:

$$I = \frac{1}{2} \sum_i (c_i z_i^2), \quad (29)$$

In this equation  $c_i$  is the molality of an ion  $i$ .

The IAP and the amounts of calcium carbonate precipitate were obtained by solving these simultaneous equations using a mathematical computer program (Mathcad® 8, Mathsoft, Inc.).

## References

- 1 S. E. Ingle, *Mar. Chem.*, **3**, 301 (1975).
- 2 J. W. Morse, F. T. Mackenzie, "Geochemistry of Sedimentary Carbonates: Developments in Sedimentology 48," Elsevier, (1990), Chapter 4–6, 133.
- 3 R. M. Pytkowicz, *J. Geol.*, **73**, 196 (1965).
- 4 R. A. Berner, *Science*, **153**, 188 (1966).
- 5 J. W. Morse, A. Mucci, L. M. Walter, M. S. Kaminsky, *Science*, **205**, 904 (1979).
- 6 E. Suess, *Geochim. Cosmochim. Acta*, **34**, 157 (1970).
- 7 T. Akagi, Y. Kono, *Aquatic Geochem.*, **1**, 231 (1995).
- 8 J. W. Morse, F. T. Mackenzie, "Geochemistry of Sedimentary Carbonates: Developments in Sedimentology 48," Elsevier (1990), Chapter 1, 1.
- 9 Y. Kitano, N. Kanamori, *Geochem. J.*, **1**, 1 (1966).
- 10 S. G. Terjesen, O. Erga, G. Thorsen, A. Ve, *Chem. Engn. Sci.*, **14**, 277 (1961).
- 11 T. Ogino, T. Suzuki, K. Sawada, *Geochim. Cosmochim. Acta*, **51**, 2757 (1987).
- 12 A. G. Xyla, P. G. Koutsoukos, *J. Chem. Soc., Faraday Trans. 1*, **83**, 1477 (1987).
- 13 E. K. Giannimaras, P. G. Koutsoukos, *J. Colloid Interface Sci.*, **116**, 423 (1987).
- 14 E. K. Giannimaras, P. G. Koutsoukos, *Langmuir*, **4**, 855 (1988).
- 15 Y. Kitano, *Bull. Chem. Soc. Jpn.*, **35**, 1973 (1962).
- 16 Y. Kitano, D. W. Hood, *Geochim. Cosmochim. Acta*, **29**, 29 (1965).
- 17 G. Falini, S. Albeck, S. Weiner, L. Addadi, *Science*, **271**, 67 (1996).
- 18 J. L. Bischoff, *Am. J. Sci.*, **266**, 80 (1968).
- 19 N. Spanos, P. G. Koutsoukos, *J. Cryst. Growth*, **191**, 783 (1998).
- 20 T. Moeller, N. Fogel, *J. Am. Chem. Soc.*, **73**, 4481 (1951).
- 21 J. H. Lee, R. H. Byrne, *Geochim. Cosmochim. Acta*, **56**, 1127 (1992).
- 22 E. Sass, J. W. Morse, F. J. Millero, *Am. J. Sci.*, **283**, 218 (1983).
- 23 L. N. Plummer, E. Busenberg, *Geochim. Cosmochim. Acta*, **46**, 1011 (1982).
- 24 A. Katsifaras, N. Spanos, *J. Cryst. Growth*, **204**, 183 (1999).
- 25 S. Zhong, A. Mucci, *Geochim. Cosmochim. Acta*, **59**, 443 (1995).